THE EXTREMELY LUMINOUS SUPERNOVA 2006gy AT LATE PHASE: DETECTION OF OPTICAL EMISSION FROM SUPERNOVA [1]

Koji S. Kawabata[2], Masaomi Tanaka [3,4], Keiichi Maeda [4,5], Takashi Hattori [6], Ken'ichi Nomoto [4,3], Nozomu Tominaga [7,3], and Masayuki Yamanaka [2,8]

Accepted for publication in the Astrophysical Journal

ABSTRACT

Supernova (SN) 2006gy is an extremely luminous Type IIn SN characterized by the bright peak magnitude $M_R \sim -22$ mag and its long duration. The mechanism giving rise to its huge luminosity is still unclear. We performed optical spectroscopy and photometry of SN 2006gy at late time, ~ 400 days after the explosion, with the Subaru/FOCAS in a good seeing condition. We carefully extracted the SN component, although there is an ambiguity because of the contamination by bright nucleus of the host galaxy. We found that the SN faded by ~ 3 mag from ~ 200 to ~ 400 days after the explosion (i.e., by ~ 5 mag from peak to ~ 400 days) in R band. The overall light curve is marginally consistent with the ^{56}Ni heating model, although the flattening around 200 days suggests the optical flux declined more steeply between ~ 200 and ~ 400 days. The late time spectrum was quite peculiar among all types of SNe. It showed many intermediate width (~ 2000 km s^{-1} FWHM) emission lines, e.g., [Fe II], [Ca II], and Ca II. The absence of the broad [O I] 6300, 6364 line and weakness of [Fe II] and [Ca II] lines compared with Ca II IR triplet would be explained by a moderately high electron density in the line emitting region. This high density assumption seems to be consistent with the large amount of ejecta and low expansion velocity of SN 2006gy. The Hα line luminosity was as small as $\sim 1 \times 10^{39}$ erg s^{-1}, being comparable with those of normal Type II SNe at similar epochs. Our observation indicates that the strong CSM interaction had almost finished by ~ 400 days. If the late time optical flux is purely powered by radioactive decay, at least $M(^{56}\text{Ni}) \sim 3 M_\odot$ should be produced at the SN explosion. In the late phase spectrum, there were several unusual emission lines at 7400–8800 Å and some of them might be due to Ti or Ni synthesized at the explosion.

Subject headings: supernovae: general — supernovae: individual (SN 2006gy)

1. INTRODUCTION

Supernova (SN) 2006gy is an extremely luminous SN found by Quimby (2006) near the nucleus of the host galaxy NGC 1260 [$\mu = (m - M) = 34.45$ mag]. Its absolute magnitude reaches ~ -22 mag (Ofek et al. 2007; Smith et al. 2007), being more luminous than typical Type Ia supernovae by a factor of ~ 10. The SN was referred to as "the most luminous SN" at that time [9]. In addition to the high peak luminosity, the light curve (LC) of SN 2006gy evolves very slowly, peaking at $t \sim 70$ days after the explosion (hereafter, t means time after the explosion) [10]. The total radiation energy exceeds 1×10^{51} ergs, i.e., comparable to the kinetic energy of typical SNe. The optical spectra of SN 2006gy show Type IIn-like features, i.e., narrow emissions of H Balmer lines.

For a model of SN 2006gy, a 'Type IIa' scenario (hybrid of Type IIn and Ia SN, like SNe 2002ic and 1997cy; Deng et al. 2004), i.e., Type Ia SN in a dense circumstellar medium (CSM), has been suggested. However, the radiation energy of SN 2006gy is comparable to (or overwhelming) the kinetic energy of Type Ia SNe so that this scenario seems unlikely (Ofek et al. 2007; Smith et al. 2007). The progenitor of SN 2006gy should be a massive star.

The source of the huge optical luminosity is under debate. Possible mechanisms are (i) thermal emission from hydrogen recombination front, (ii) interaction between CSM and SN ejecta, and (iii) radioactive decay of ^{56}Ni . Ofek et al. (2007) suggested that the luminosity comes from the CSM interaction, as in Type IIn/IIa SNe. On the contrary, Smith et al. (2007) suggested that radioactive decay is the primal (or least problematic) heating source, because only weak X-rays were detected from SN 2006gy

(suggesting CSM interaction was not strong) and the observed expansion velocity of hydrogen envelope was unusually slow (suggesting too small emitting radius for thermal radiation). Agnoletto et al. (2009) gave an idea that the massive CSM was clumpy and both the CSM interaction and the radioactive decay contributed to the enormous luminosity. Furthermore, Smith et al. (2007) suggested that SN 2006gy is a pair-instability SN (PISN) because a huge amount of ^{56}Ni ($> 10 M_\odot$) is required to explain the peak luminosity. However, Nomoto et al. (2007) shows that the LC of the PISN model evolves too slowly to reproduce the observed LC. Umeda & Nomoto (2008) explored a possibility that core-collapse SNe could synthesize such a large amount of ^{56}Ni.

Woosley, Blinnikov & Heger (2007) showed that the collision between the shells ejected by pulsational pair instability in massive stars initially having $\sim 90 M_\odot$ could reproduce the peak luminosity of SN 2006gy. Smith & Mc-Cray (2007) also presented a simple "shell-shocked" model involving shock-deposited energy as the heat source. In these two models, the shell is so thick that X-rays are absorbed. Portegies Zwart & van den Heuvel (2007) suggested that the SN 2006gy was an outcome of merging between two massive stars in a dense and young cluster, being consistent with presence of a large amount of hydrogen.

Recently, Smith et al. (2008a) presented results of late phase observations ($t = 362$–468 days). The SN was clearly seen in NIR images obtained with the adaptive optics on the Keck II telescope, while any optical observation failed to detect the SN component even for Hα emission. The NIR flux would be attributed to newly-formed dust particles or an IR echo. Agnoletto et al. (2009) also successfully detected this SN in K band at $t = 411$–510 days, but failed to detect the SN in the optical bands at $t = 389.5$–423.5 days.

In this paper, we report on the results of our late time observation ($t = 394$ days) of SN 2006gy with the Subaru telescope. The late phase luminosity and spectra may give clues to distinguish the underlying scenarios as also mentioned by Smith et al. (2008a). In §2, we describe our observations and data reduction. In §3, the LC of SN 2006gy is compared with those of other SNe and results of model calculations. In §4, the spectra of SN 2006gy are analyzed. Features in the late phase spectrum is further investigated by comparing it with spectra of SNe of various types (§5). Finally we give conclusions in §6.

2. OBSERVATIONS AND DATA REDUCTION

The observations were carried out with the Faint Object Camera And Spectrograph (FOCAS, Kashikawa et al. 2002). FOCAS is an optical versatile instrument attached to the Cassegrain focus of the 8.2-m Subaru telescope. The images were recorded on two MIT/LL CCDs (2k×4k, 15 μm pixel^{-1}). To minimize the harmful effect due to atmospheric dispersion in observation at low altitude, we used the Atmospheric Dispersion Corrector (ADC) in front of FOCAS, which reduces the chromatic elongation to less than $0\rlap{.}''1$ within wavelengths 3500–11000 Å at airmass ≤ 2.0. We took all images at airmass less than 1.9 (Table 1), which promises that the effect was negligible in our observations.

For spectroscopy, we obtained high resolution spectra ($R \simeq 3600$) on 2006 Dec 25.4 ($t = 127$ days) and 2007 Jan 24.4 ($t = 157$ days) and a low resolution spectrum ($R \simeq 660$) on 2007 Sep 18.5 ($t = 394$ days). For the high resolution spectroscopy, we used a $0\rlap{.}''4$ width slit, a 665 lines mm^{-1} volume-phase holographic grism and SY47 order-cut filter, which gives a wavelength coverage of 5300–7700 Å and a spectral resolution of $\simeq 1.8$Å . For the low resolution one, we used a $0\rlap{.}''8$ width offset-slit, a 300 lines mm^{-1} blue grism and SY47 filter, giving a wavelength coverage of 4800–9000 Å and a spectral resolution of $\simeq 9.6$Å . The total exposure time was 1200 s on each night. The direction of the slit was set to position angle (PA) $-75°$ to take spectra of both the nucleus of the host galaxy NGC 1260 and the SN simultaneously. Flux calibration and the correction for atmospheric absorption bands were performed using spectra of a spectrophotometric standard star obtained on the same night; BD $+28°4211$ in 2006 Dec, Feige 34 in 2007 Jan and G191B2B in 2007 Sep. The log of observation is shown in Table 1.

For photometry, we took V and R band images just before the spectroscopy. The exposure times of V and R bands are 3 s and 4 s in 2006 Dec, 5 s and 5 s in 2007 Jan and 10 s and 10 s in 2007 Sep, respectively. We used 2×2 on-chip binning in the CCD readout and the resultant scale was $0\rlap{.}''208$ per a binned-pixel. The magnitude of the SN is calibrated with Landolt field stars (Landolt 1992).

2.1. Background subtraction

Since the SN was very close to the bright nucleus of the host galaxy ($\Delta \simeq 0\rlap{.}''9$), the subtraction of the background component should be carefully performed, especially for late phase data.

In the earlier phase data, the SN was sufficiently bright and the artificial error originated in the adopted method for the background subtraction is not significant. For photometry, we subtracted PSF-matched 394 days image in the same band as the background, and then performed PSF-photometry. Although this method gives an over-subtraction due to a non-negligible SN component at $t = 394$ days, the error should be small (~ 0.03 mag) because the SN faded by about 4 mag between $t = 127$ days and 394 days. The photometric error was derived from the root sum square of the magnitude transformation error using the Landolt field stars and the photon noises of the SN and the background. For spectroscopy, we assumed that the two-dimensional (2D) spectral image of the host galaxy is symmetric across the nucleus, and simply subtracted the mirrored spectral image across the nucleus.

For the late phase data, we should mention at first that the SN component was successfully detected in both imaging (Fig. 2) and spectroscopic (Fig. 3a-d) data, although Smith et al. (2008a) and Agnoletto et al. (2009) reported their null detection in optical data between $t = 364$ and $t = 423.5$ days. We assume that the better seeing condition at our observation enabled us to distinguish the SN component from the host galaxy nucleus. However, it is still a difficult task to derive the intrinsic SN component because the background galaxy has inhomogeneous structures. For photometry on $t = 394$ days, we assumed a symmetry for the brightness distribution of the host galaxy

with respect to its polar axis (PA$\simeq -8°$) and adopted the mirrored image as the background for the lack of better alternatives. In the background-subtracted image, the SN is seen nearly as a point-like source embedded in a diffuse elongated component (Fig 2). The PSF-photometry for the SN and nearby two stars (C1 and C2 in Fig. 2) provided $V = 20.77 \pm 0.17$ and $R = 19.36 \pm 0.14$ for the SN, $V = 19.48 \pm 0.14$ and $R = 18.37 \pm 0.13$ for C1 and $V = 20.51 \pm 0.16$ and $R = 19.77 \pm 0.14$ for C2. Our preliminary aperture-photometry with several parameter sets (radii of stellar aperture and sky annulus) gave somewhat scattered values for the SN magnitudes, $V = 20.7 \pm 0.4$ and $R = 19.4 \pm 0.4$, because of the inhomogeneous background. To check the reliability of the uncertainty, we added an artificial star having the same brightness at several positions near the SN and performed photometry of it. The result of this test was consistent with above photometry and we adopt $V = 20.7 \pm 0.4$ and $R = 19.4 \pm 0.4$ as the SN magnitude. It is noted that these magnitudes might be contaminated by unresolved background components, e.g., H II regions and/or stellar clusters in the host galaxy, and thus they should be considered as the brighter limits.

In the spectroscopic data, we estimated the background component using the neighboring regions on both sides of the SN position, BG1 and BG2 along the slit (Fig. 1 and 3). Since the simple mean of BG1 and BG2 spectra clearly leads to over-estimation of the background component (i.e., spatial distribution of the background component is no longer linear along the slit), we scaled the BG1 and BG2 spectra to match the SN flux at apparently line-free region, 7814–7856 Å rest wavelength before the averaging. The scaling factors and the scaled spectra of BG1, BG2 and some other regions are shown in Figures 4a. Four background spectra (BG1, BG2, galaxy core and mirror position) resemble to one another and they are well explained by a slightly reddened bulge spectrum (Bruzual & Charlot 2003). From these spectra (including 2D spectral images in Figure 3) we recognize the existence of [Fe II] 7155, [Ca II] 7300 and Ca II IR triplet emission lines in the SN spectrum. The enlarged spectra around Hα line (Fig. 4b) also implies the presence of an intermediate-width (15–30Å $\simeq$ 700–1400 km s^{-1}) Hα emission line. They are discussed later. Finally, we adopted the mean of the scaled BG1 and BG2 spectra as the background component, and then subtracted it from the SN position spectrum to derive the pure SN spectrum. This method leads to complete elimination of the continuum component of the SN, at least, around the line-free regions. The resultant SN spectrum provides the faint-end limit of the magnitude of the SN as $V \lesssim 21.7$ and $R \lesssim 21.1$ (as far as we ignore the contamination by the possible unresolved component as mentioned above), which are consistent with the results of our photometry. It is noted that there is a non-negligible difference between the normalized BG1 and BG2 spectra, especially at bluer wavelengths, which may lead to a large uncertainty for the resultant SN flux at $t = 394$ days up to $\pm 60\%$ (Fig. 5). This uncertainty is larger than the error of estimated extinction toward the SN (see §4). In this paper we mainly discuss the emission line components at longer than 5800 Å for the late phase spectrum and therefore this uncertainty does not affect our discussion.

3. LIGHT CURVE ANALYSIS

Figure 6 shows the R band light curve (LC) of SN 2006gy constructed from the published data (Smith et al. 2007; Agnoletto et al. 2009) and our Subaru ones. It is compared with bright Type Ic SN 1998bw (Patat et al. 2001) and Type IIa SN 2002ic (Deng et al. 2004) and Type IIn SN 1999el (Di Carlo et al. 2002). There exists a large variety among the LCs of Type IIa and IIn SNe. The LC of SN IIa 2002ic declines very slowly.[11] The slope is flatter than that the LC powered by the ^{56}Co $\rightarrow$ ^{56}Fe decay with fully trapped γ-rays. This behavior is also seen in other SNe, e.g., SN IIa 1997cy and SN IIn 1988Z (e.g., Germany et al. 2000; Turatto et al. 1993; Turatto et al. 2000). On the other hand, the LC of SN 1999el declines faster than SNe 2002ic and 1998bw. Similar behavior is also seen in the LC of Type IIn SN 1998S (Fassia et al. 2000). In another Type IIn SN 1994W, a sudden decline of the LC was observed after ~ 100 days plateau (Sollerman, Cumming & Lundqvist 1998, Chugai et al. 2004). The main heating source of Type IIn and IIa SNe is thought to be the interaction between SN ejecta and CSM (e.g., Turatto et al. 1993; Chugai et al. 2004), and this heterogeneity in the LC may reflect the structure, the mass and the kinetic energy of the SN ejecta as well as the structure (density and its slope) of CSM.

In contrast to Type IIn SNe, the LCs of SNe where ^{56}Ni is the dominant heating source show similar shapes. The LC declines faster than the ^{56}Co decay line because a fraction of γ-rays escape without interacting with the SN ejecta. The deviation from the ^{56}Co decay line gradually becomes larger because the expanding SN ejecta gets thinner against γ-rays. The LC of Type Ic SN 1998bw is fully explained by this scenario (Patat et al. 2001; Maeda et al. 2003).

The early LC of SN 2006gy tends to be leveled around $t = 200$ days. Our Subaru data shows that the LC fades by ~ 3 mag from $t \sim 200$ to ~ 400 days, which is consistent with the results of NIR photometry at $t = 405$ and 468 days (Smith et al. 2008a). The decline rate during this period is clearly faster than that of SN 2002ic and the ^{56}Co decay line, while it seems comparable to that of SN 1998bw. In other words, the LC of SN 2006gy does not show any particularly peculiar behavior that is not explained by the ^{56}Co decay. However, we cannot exclude the possibility that the LC is almost leveled at $t \sim 200 - 350$ days and suddenly declines just before $t \sim 394$ days.

In the right panel of Figure 6, the ^{56}Ni+ ^{56}Co decay model presented by Nomoto et al. (2007) is also shown. They computed a bolometric LC and showed that the model with $M_{ej} = 53 M_{\odot}$, $E_K = 64 \times 10^{51}$ erg and $M(^{56}\text{Ni}) = 15 M_{\odot}$ explains the observed LC up to $t \sim 200$ days. Here M_{ej}, E_K and $M(^{56}\text{Ni})$ are the mass of the ejecta, the kinetic energy of the ejecta, and the mass of ^{56}Ni ejected by the explosion, respectively. The model LC is in reasonably good agreement with our late phase observation.

If we assume that the radioactive decay is the main energy source of emission at $t = 394$ days, $M(^{56}\text{Ni}) \gtrsim 3 M_{\odot}$

---

[11] We assume that the explosion date is 2002 Nov 3 (Hamuy et al. 2003) although it is unclear and an exact LC comparison is not easy.

is needed to explain the R band flux. Although the model LC for SN IIa 2002ic (Nomoto et al. 2005) is not consistent with that of SN 2006gy, we cannot preclude the CSM interaction model because of the large diversity of LCs in Type IIn/IIa SNe. We note that the model by Woosley et al. (2007) is also consistent with our observation. However, the diffusion model by Smith & McCray (2007), predicting a fast decline after the maximum (~ -13 mag at $t = 300$ days), is inconsistent with our data. Also, the LCs of the PISN model (blue dashed line) is not consistent with the observed LC.

4. SPECTRAL ANALYSIS

The spectra of SN 2006gy are shown in Figure 7, and closed-up profiles of some lines are shown in Figure 8. The redshift $z = 0.01967$, derived from the diffuse Hα emission line of the host galaxy (cf. $z = 0.01910$ derived at the nucleus), has been corrected for. We assumed the total extinction of $E(B-V) = 0.628 \pm 0.094$ (or $A_R = 1.68 \pm 0.25$) toward the SN, which is the sum of the extinction in the Milky Way [$E(B-V) = 0.16$; Schlegel, Finkbeiner, & Davis 1998] and that within the host galaxy [$E(B-V) = 0.468 \pm 0.094$, derived from $A_R = 1.25 \pm 0.25$ and $A_{\text{Landolt } R} = 2.673 \times E(B-V)$; Smith et al. 2007, Schlegel et al. 1998]. The equivalent width (EW) of the Galactic Na I $D_1 D_2$ absorption lines in our high resolution spectrum (EW= 1.2 Å) is almost consistent with $E(B-V) = 0.16$ using an empirical relation of $E(B-V) = -0.01 + 0.16 \times EW(\text{Å})$ suggested by Turatto, Benetti, & Cappellaro (2003). Although the EW of the host galaxy Na I D line in the same spectrum suggests a larger extinction within the host galaxy ($E(B-V) \sim 1$), it should be partly circumstellar origin because some of other spectral features (Hα and Fe II) are accompanied with narrow absorption components in their P-Cyg type profiles. Our late time spectrum suffers from large uncertainty in the EW of Na I D line because of the faint SN spectrum and the uncertain continuum level (see §2.1).

Like other Type-IIn SNe, our early phase spectra of SN 2006gy are characterized by a strong Hα emission line as well as many Fe II, He I and Na I lines. As shown in Figure 8, the Hα emission line in the spectra at $t = 127$ days has a narrow P-Cyg type component near the peak, of which the marginally resolved emission line has a width of ~ 120 km s^{-1} FWHM, and a broad wing component exceeding ± 5000 km s^{-1}. The broad component is clearly asymmetric, being brighter in the red wing than in the blue. Smith et al. (2007) took a high-resolution spectrum at $t = 96$ days ($R \approx 4500$) and suggested that the asymmetric profile is produced by broad absorption component at the blue side. This component had a sharp blue edge at ~ -4000 km s^{-1}, which is considered to be an effective speed of the SN blast wave (Smith et al. 2007). This asymmetric profile was seen through $t = 157$ days, although the absorption component became less significant. For some features, e.g., Fe II 5535 and Na I D at $t = 127$ days, broad blue-shifted absorption components up to $4000 - 5000$ km s^{-1} are also significant (Fig. 7). The narrow absorption component of the Hα peak considerably evolved from $t = 96$ to 157 days. It splits into possible double components by 127 days, and the whole width between both edges of the absorption fea-

ture increased from 260 km s^{-1} to 690 km s^{-1} . These suggest an ongoing interaction between the ejecta and the dense CSM.

In the late phase spectrum (Fig. 5), we can see several emission lines, mainly in red wavelengths, including [Ca II] 7291, 7323 (7302 in average), Ca II IR triplet and [Fe II] 7155, which are listed in Table 2. On the other hand, the bluer spectrum is likely to be dominated by continuum component and/or heavily blended emission lines. A broad absorption trough (up to -5000 km s^{-1}) possibly belonging to Na I D is significant in this region. Additionally, as mentioned in §2.1, there is a possible Hα emission line having an intermediate-width (700–1400 km s^{-1}). If the flux excess at the minimum point (6574 Å) between Hα and [N II] 6584 lines is actually due to the intermediate-width Hα component (Fig. 4b), its observed flux is derived to be $\simeq 6 \times 10^{-17}$ erg s^{-1} cm^{-2} Å^{-1} above the continuum level of $\simeq 5 \times 10^{-17}$ erg s^{-1} cm^{-2} Å^{-1}. This continuum flux is consistent with the upper-limit ($\lesssim 2 \times 10^{-17}$ and $\lesssim 9 \times 10^{-17}$ erg s^{-1} cm^{-2} Å^{-1} before and after the extinction-correction, respectively) set by Smith et al. (2008a). Assuming that the flux excess is actually due to an Hα line of which the line width is ~ 20 Å, we can derive the luminosity of the line flux as $\sim 1 \times 10^{39}$ erg s^{-1}.

In Figures 9–11, the late time spectrum of SN 2006gy is compared with those of various classes of SNe. Unlike other slowly-declining Type IIn/IIa SNe, the Hα emission line is neither strong nor wide. The emission of Ca II IR triplet in SN 2006gy is much narrower than those in other Type IIn/IIa SNe, suggestive of a slow SN ejecta. The presence of forbidden lines [Fe II] 7155 and [Ca II] 7302 is also peculiar for a Type IIn/IIa SN. On the other hand, this SN does not show strong [O I] 6300, 6364 emission line, which is generally strong in Type II and Ib/c SNe having forbidden [Ca II] 7302 line (Fig. 9 and 11)[12]. Some of the intermediate-width emission lines, marked with dashed lines in Figure 5, are unusual for any type of SNe. The presence of the wide absorption trough at Na I D is also unusual for Type IIn/IIa SNe. Similar feature is seen in the late phase spectrum of a peculiar Type Ia SN 2005hk (Fig. 11). We discuss these peculiar properties of SN 2006gy in the next section.

5. DISCUSSION

5.1. *CSM Interaction or Radioactive Decay Heating?*

The luminosity of SN 2006gy at the late phase is consistent with the radioactive decay model as shown in Figure 6. The LCs of Type IIn SNe show a large variety and some of which might also be in fair agreement with SN 2006gy. Thus, it seems difficult to discriminate the main heating source of SN 2006gy only from the LC. The late time spectrum gives some indications on this issue.

SN 2006gy is classified as Type IIn from earlier spectra showing strong Hα emission line. However, as mentioned in §4, the late time spectrum is quite atypical for Type IIn/IIa SNe (Fig. 10). The emission lines of Ca II IR triplet are narrow and not blended. There are several forbidden lines, e.g., [Fe II] 7155 and [Ca II] 7302. The luminosity of the possible Hα emission line at 394 days ($\sim 1 \times 10^{39}$ erg s^{-1}) is considerably smaller than those

---

[12] The [O I] line is also absent in Type Ia SNe because of the low oxygen abundance in the ejecta (see e.g., Kozma et al. 2005)

of Type IIn SNe 1988Z (2.0×10^{41} erg s^{-1} at 492 days; Turatto et al. 1993), 1995Z (3.2×10^{40} erg s^{-1} at 716 days; Fransson et al. 2002) and 2006tf (7.9×10^{40} erg s^{-1} at 445 days after discovery; Smith et al. 2008b) and also Type IIa SN 2002ic at earlier phase [$(2 - 3) \times 10^{41}$ erg s^{-1} at 222 days; Deng et al. 2004]. It is rather consistent with the pure radioactive decay model of a typical type II SN (~ 0.1 M$_\odot$ ^{56}Co and ~ 10 M$_\odot$ envelope; Chugai 1991). Thus, the observed Hα emission flux does not require any Type IIn-like CSM interaction at $t = 394$ days. Therefore, the strong CSM interaction expected from the conspicuous Hα emission and the flattened LC before ~ 200 days seems to have faded by 394 days. If the observed R band luminosity is purely originated from radioactive decay, $M(^{56}\mathrm{Ni}) \gtrsim 3 M_\odot$ is necessary as discussed in §3.

However, the pure radioactive decay model also seems to have an inconsistency. Core-collapse SNe generally show the [O I] 6300, 6364 line at late time except for Type IIn/IIa SNe, while SN 2006gy showed little or no [O I] emission (Figs. 9–11). As for Fe lines, in Type Ic SN 1998bw, a blend of [Fe II] lines is seen around 5200 Å and the [Fe II] 7155 line has a dominant contribution to the emission line around 7200 Å, while only [Fe II] 7155 line is seen in SN 2006gy. The LC of SN 1998bw is fully explained by the heating of $\sim 0.4 M_\odot$ of ^{56}Ni (Iwamoto et al. 1998; Nakamura et al. 2001; Maeda et al. 2006). If the peak luminosity of SN 2006gy is powered by the decay of ^{56}Ni, the required mass of ^{56}Ni is $\gtrsim 10 M_\odot$, more than 20 times larger than that of SN 1998bw. This would result in stronger Fe lines in SN 2006gy. The same discussion holds true in comparison with Type Ia SNe, which eject $\sim 0.6 M_\odot$ of ^{56}Ni on average (e.g., Stritzinger et al. 2006). Both SNe 1990N and 2004eo showed strong and broad [Fe II] features around 5200 Å and 7150 Å (Fig. 11). Thus, the weakness of [O I] and [Fe II] lines seem against the ^{56}Ni heating scenario. However, this peculiarity in the line strength might be explained by a moderately high density of the line emitting region. We will discuss it in §5.2.

5.2. *Moderately High Density of Line Emitting Region*

The presence of the forbidden [Fe II] 7155 and [Ca II] 7302 lines suggests the density of the emitting region in SN 2006gy is less than those in other Type IIn/IIa SNe. However, it is likely that the density is still higher than those of other type SNe; the line flux ratio $F(7302)/F(\text{IR triplet})$ of SN 2006gy is only $\simeq 0.5$ (Table 2), while $F(7302)/F(\text{IR triplet}) > 1$ in SNe of other types (Fig. 9 and 11; see also Gómez & López 2000).

The value of $F(7302)/F(\text{IR triplet}) \simeq 0.5$ suggests an electron density of the emitting region $N_e \simeq 10^8$–10^9 cm^{-3} (Ferland & Persson 1989; Fransson & Chevalier 1989). This is consistent with the existence of the [Fe II] 7155 because its critical density of electron is not so small (a few times 10^8 cm^{-3}; Zickgraf 2003). In such a high density region, the forbidden line [O I] 6300, 6364 would be effectively quenched, because its critical density is only a few times 10^6 cm^{-3}. Therefore, the low $F(7302)/F(\text{IR triplet})$ value and the absence of [O I] 6300, 6364 in SN 2006gy can be qualitatively explained by a moderately high electron density of the emitting region, which would be less than those of Type IIn/IIa SNe and more than other Type II

and Ib/c SNe.

In such a high density environment, emission could occur in permitted Fe II multiplets (e.g., Turrato et al. 2000; Deng et al. 2004), which might contribute to the blue continuum flux at $\lambda \lesssim 6000$ Å. The absence of intermediate-width [Fe II] line around 5200 Å , which is seen together with [Fe II] 7155 in Type Ia SNe as well as in the peculiar Type Ic SN 1998bw (Fig. 11), might be explained by this higher density assumption.

The high density of the ejecta is also consistent with the current understanding that the ^{56}Ni heating model requires a massive progenitor and a large amount of ejecta (Umeda & Nomoto 2008). A large ejecta mass is also needed to reproduce the long duration of the LC around maximum. The high density of the ejecta would also be consistent with the lower expansion velocity (~ 1000 km s^{-1}) derived from FWHM of the emission lines in the late time spectrum. Low expansion velocity was also suggested from early spectroscopy (Ofek et al. 2007).

5.3. *Unusual Emission Lines: From Inner Ejecta?*

There are several unusual features in the late time spectrum of SN 2006gy (marked with dashed lines in Fig. 5). These lines are not clearly seen in other types of SNe (Fig. 9–11). Consulting line lists in literature (e.g., Moore 1945), we find possible candidates as shown in Table 2. Some of them could be lines of nickel ([Ni II] 7380, 8704; [Ni I] 7394, 7908, 8202, 8843) and/or titanium ([Ti II] 7917, 8040, 8060, 8349, 8371). The emission line at 7716 Å could be due to iron ([Fe I] 7709 or [Fe II] 7765).

If these identifications are correct, the innermost ejecta of SN 2006gy was visible at $t = 394$ days because Ni and Ti are likely to exist only inner part of the ejecta. Assuming that the line emitting region expands homologously with 1000 km s^{-1} and all the elements are singly ionized, the high density (10^8 cm$^{-3} \lesssim n_e \lesssim 10^9$ cm^{-3}) implies that the mass of the hypothetical innermost region is ~ 0.8–$8 M_\odot$ (if dominated by Fe-peak elements) or ~ 0.3–$3 M_\odot$ (if dominated by Ca). This would suggest that the assumption of $n_e \lesssim 10^9$ cm^{-3} is reasonable. In this case, the electron scattering optical depth is ~ 0.2–2, which suggests that $n_e \lesssim 10^9$ is also necessary for the innermost region to be optically thin. In sum, our hypothesis of the emergence of the innermost part requires $n_e \lesssim 10^9$ cm^{-3}, being consistent with the high density interpretation.

However, the identification of these lines are still tentative. For example, we do not see the [Ni I] 7507 feature in the observed spectrum (Fig. 5), although it is expected to emit as strong as the [Ni I] 7908. It is noted the feature around 7910 Å is also seen in some Type Ia SNe (Fig. 11). There is also an overall resemblance with the peculiar Type Ia SN 2005hk at 240 days, especially at 5500–6000 Å , 7100–7500 Å and 8500–8900 Å (Fig. 11). To discuss this subject further, a more reliable identification of these lines will be needed.

6. CONCLUSIONS

We presented the spectroscopic and photometric observation of luminous Type IIn SN 2006gy at $t = 394$ days. The good seeing condition enabled us to detect it in the optical wavelengths. The overall LC is roughly consistent with the radioactive heating model. The deviation

between the observed LC and the radioactive LC model around 200 days suggests that the strong CSM interaction considerably contributed at ~ 200 days and then weakened by 394 days.

The late time spectrum of SN 2006gy was unique. It showed some emission lines with intermediate width ($\sim 2000\,\mathrm{km\,s^{-1}}$), including forbidden lines of [Fe II] and [Ca II] which are not seen in normal Type IIn/IIa SNe. The absence of [O I] 6300, 6364 line and the weakness of [Fe II] lines would be a result of moderate electron density of $\simeq 10^8$–10^9 cm^{-3} in the emission line region. This is consistent with the larger amount of ejecta and less expansion velocity suggested for this SN. Although SN 2006gy exhibited possible Hα emission line, its flux was considerably lower than those of Type IIn/IIa SNe and rather comparable with that of a typical Type II SN. This suggests that the strong CSM interaction has finished by $t = 394$ days, being consistent with the prediction from the LC.

Several unusual emission features were present at 7400–8800Å and some of them might be Ni and/or Ti lines. However, these identifications are still tentative and we need detailed modeling to explain the full aspects of the observation.

REFERENCES

Agnoletto, I., et al. 2009, ApJ, in press (arXiv: 0810.0635)
Barbon, R., Benetti, S., Cappellaro, E., Patat, F., Turatto, M., & Iijima, T. 1995, A&AS, 110, 513
Bruzual, G., & Charlot, S. 2003, MNRAS, 344, 1000
Chugai, N. N. 1991, MNRAS, 250, 513
Chugai, N. N., et al. 2004, MNRAS, 352, 1213
Di Carlo, E., et al. 2002, ApJ, 573, 144
Deng, J., et al. 2004, ApJ, 605, 37
Fassia, A., et al. 2000, MNRAS, 318, 1093
Ferland, G. J., & Persson, S. E. 1989, ApJ, 347, 656
Fransson, C., et al. 2002, ApJ, 572, 350
Fransson, C., & Chevalier, R. A. 1989, ApJ, 343, 323
Germany, L.M., Reiss, D.J., Sadler, E.M., Schmidt, B.P., & Stubbs, C.W. 2000, ApJ, 533, 320
Gezari, S., et al. 2009, ApJ, 690, 1313
Gómez, G., & López, R 1998, AJ, 115, 1096
Gómez, G., & López, R 2000, AJ, 120, 367
Hamuy, M., et al. 2003, Nature, 424, 651
Iwamoto, K., et al. 1998, Nature, 395, 672
Kashikawa, N., et al. 2002, PASJ, 54, 819
Kozma, C., Fransson, C., Hillebrandt, W., Travaglio, C., Sollerman, J., Reinecke, M., Röpke, F. K., & Spyromilio, J. 2005, A&A, 437, 983
Landolt, A. U. 1992, AJ, 104, 340
Maeda, K., et al. 2003, ApJ, 593, 931
Maeda, K., Mazzali, P.A., & Nomoto, K 2006, ApJ, 546, 1331
Maeda, K., et al. 2008, Science, 29, 1220
Massey, P., & Gronwall, C. 1990, ApJ, 358, 344
Miller, A. A., et al. 2009, ApJ, 690, 1303
Moore, C. E. 1945, A Multiplet Table of Astrophysical Interest (Princeton: Princeton Univ. Obs.)
Nakamura, T., et al. 2001, ApJ, 550, 991
Nomoto, K., Suzuki, T., Deng, J., Uenishi, T., & Hachisu, I. 2005, in ASP Conf. Ser. 342, 1604-2004: Supernovae as Cosmological Lighthouses, ed. M. Turatto et al. (San Francisco: ASP), 105

Nomoto, K., Tominaga, N., Tanaka, M., Maeda, K., & Umeda, H. 2007, "Supernova 1987A: 20 Years After: Supernovae and Gamma-Ray Bursters", eds. S. Immler, K. Weiler, & R. McCray (New York: AIP), 412 (astroph/0707.2187)
Ofek, E.O., et al. 2007, ApJ, 659, L13
Pastorello, A. et al., 2007, MNRAS, 377, 1531
Patat, F., et al. 2001, ApJ, 555, 900
Portegies Zwart, S. F., & van den Heuvel, E. P. J. 2007, Nature, 450, 388
Pozzo, M., Meikle, W. P. S., Fassia, A., Geballe, T., Lundqvist, P., Chugai, N. N., & Sollerman 2004, MNRAS, 352, 457
Pun, C.S.J., et al. 1995, ApJS, 99, 223
Quimby, R. M. 2006, CBET, 644, 1
Quimby, R. M., Aldering, G., Wheeler, J.C., Höflich, P., Akerlof, C.W., & Rykoff, E.S. 2007, ApJ, 668, L99
Sahu, D. K., Anupama, G.C., Srividya, S., Muneer, S. 2006, MNRAS, 372, 1315
Sahu, D. K., Tanaka, M., Anupama, G. C., Kawabata, K. S., Maeda, K., Tominaga, N., Nomoto, K., & Mazzali, P. A. 2008, ApJ, 680, 580
Schlegel, D. J., Finkbeiner, D. P., & Davis, M. 1998, ApJ, 500, 525
Smith, N., et al. 2007, ApJ, 666, 1116
Smith, N. & McCray, R. 2007, ApJ, 671, L17
Smith, N., et al. 2008a, ApJ, 686, 485
Smith, N., Chornock, R., Li, W., Ganeshalingam, M., Silverman, J. M., Foley, R., Filippenko, A. V., & Barth, A. J. 2008b, ApJ, 686, 467
Sollerman, J., Cumming, R.J., & Lundqvist, P. 1998, ApJ, 493, 933
Turatto, M., Cappellaro, E., Danziger, I.J., Benetti, S., Gouiffes, C., & Della Valle, M. 1993, MNRAS, 262, 128
Turatto, M., et al. 2000, ApJ, 534, L57
Turatto, M., Benetti, S., & Cappellaro, E. 2003, in From Twilight to Highlight: The Physics of Supernovae, ed. W. Hillebrandt & B. Leibundgut (Berlin: Springer), 200
Umeda, H., & Nomoto, K. 2008, ApJ, 673, 1014
Woosley, S.E., Blinnikov, S., & Heger, A. 2007, Nature, 450, 390
Zickgraf, F.-J. 2003, A&A, 408, 257

TABLE 1

LOG OF THE SPECTROSCOPIC OBSERVATIONS

Epoch[a]	UT	MJD	Res. $\lambda/\Delta\lambda$	Exposure (s)	seeing (FWHM)	Airmass	V mag	R mag
127 days	2006 Dec 25.4	54094.4	3600	1200	$1''0$–$1''1$	1.18–1.23	16.38 ± 0.1	15.38 ± 0.1
157 days	2007 Jan 24.4	54124.4	3600	1200	$1''8$–$2''2$	1.68–1.84	—	—
394 days	2007 Sep 18.5	54361.5	660	1200	$0''5$–$0''6$	1.12–1.15	20.7 ± 0.4	19.4 ± 0.4

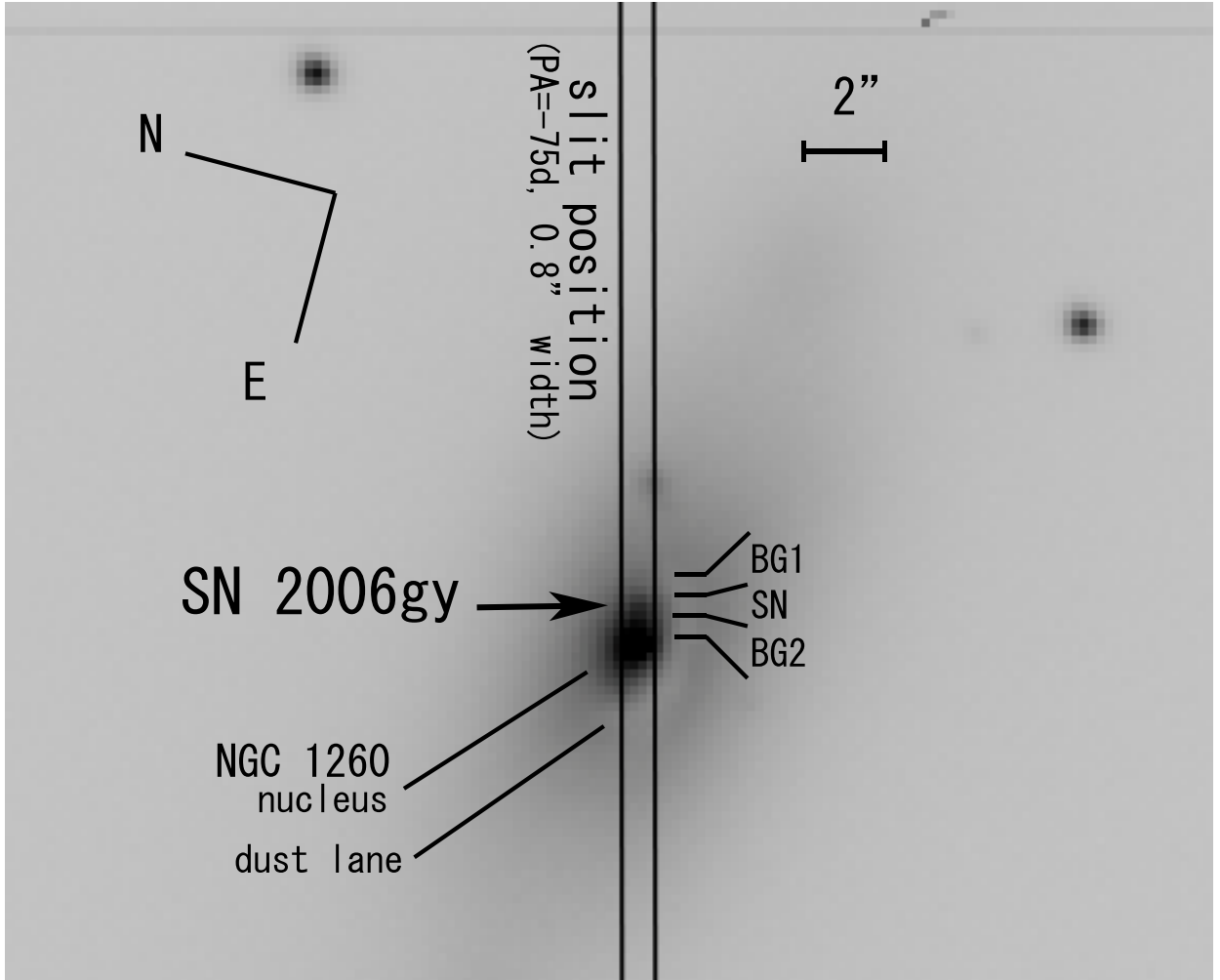[a]Rest frame days after explosion, 53967.5 MJD.

FIG. 1.— R band image obtained for the slit position alignment at the beginning of spectroscopy on 2007 Sep 18 ($t = 394$ days). We can see SN 2006gy and the nucleus of the host galaxy, NGC 1260. The SN, $\sim 0\rlap{.}''9$ apart from the center of the galactic nucleus, is marked by arrow. In the spectroscopy, the entrance slit was set as indicated by the vertical parallel lines to lie on both the SN and the galactic nucleus. We also indicate the regions which were used in one-dimensioning of the SN and the background (BG1, BG2) spectra (see §2 and §4). The seeing FWHM was $0\rlap{.}''55$ in this image.

Line center[a] (Å)	Intensity[a] (10^{15} erg s^{-1} cm^{-2})	FWHM[a] (Å)	Comment
6563?	~ 1[b]	~ 20[b]	Hα 6563
7059	1.6 ± 0.6	58 ± 8	He I 7067
7155	5.5 ± 2.2	94 ± 6	[Fe II] 7155
7302	6.0 ± 1.7	83 ± 9	[Ca II] 7291, 7323, [O II] 7320, 7330, Fe II 7308
7387	0.8 ± 0.8	40 ± 16	[Ni II] 7380?, [Ni I] 7394?
7443	4.5 ± 0.5	113 ± 15	Fe II 7462
7716	2.8 ± 0.6	117 ± 13	Fe II 7712, [Fe I] 7709?, [Fe II] 7765?
7913	2.3 ± 0.6	57 ± 7	[Ni I] 7908?, [Ti II] 7917?
8052	6.0 ± 1.5	93 ± 3	[Ti II] 8040?, [Ti II] 8060?
8206	1.3 ± 0.5	55 ± 6	[Ni I] 8202?, [Ni I] 8195?
8325	1.9 ± 0.4	62 ± 12	[Ti II] 8349?,[Fe I] 8348?
8383	1.9 ± 0.4	49 ± 8	[Ti II] 8371
8479	1.3 ± 0.3	56 ± 10	Ca II 8498, [Fe I] 8490?
8544	4.8 ± 1.2	56 ± 4	Ca II 8542
8681	5.5 ± 0.9	100 ± 7	Ca II 8662, [Ni II] 8704?
8835	3.6 ± 0.4	98 ± 7	[Ni I] 8843?

[a]Center wavelength, intensity and full-width at half-maximum of de-blended gaussian profiles from the SN spectrum are shown, except for Hα. In the de-blending the continuum level was set to zero. The errors are estimated from results of several de-blending trials for the SN spectrum (in which the mean of scaled BG1 and BG2 is subtracted) and also for other spectra (in which either only scaled BG1 or BG2 is subtracted; see Fig. 5).

[b]Assumed a constant flux 0.61×10^{-16} erg s^{-1} cm^{-2} Å^{-1} (above the continuum level of 0.52×10^{-16} erg s^{-1} cm^{-2} Å^{-1}) and a total width of ~ 20 Å(see §4).
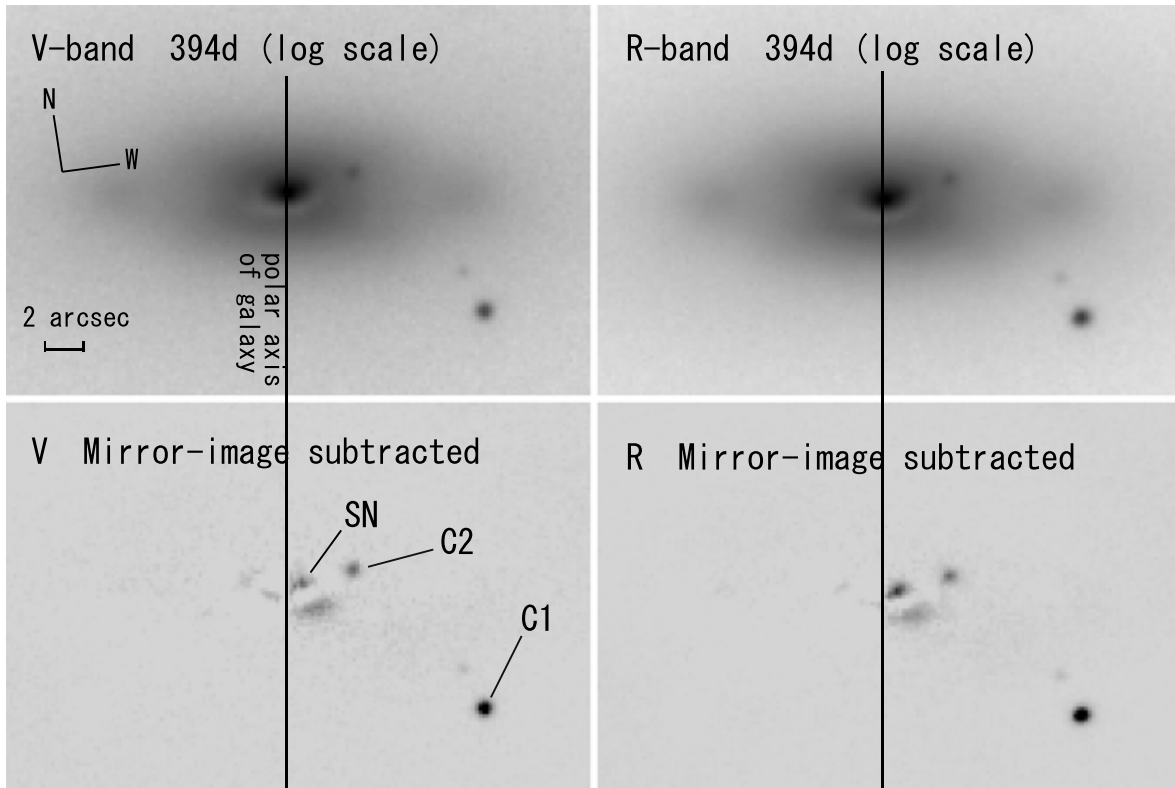

FIG. 2.— (Upper) V and R band images obtained by Subaru/FOCAS at $t = 394$ days. The images are rotated to align the polar axis of the host galaxy (PA$= -8°$) to the vertical axis as shown. (Lower) Background-subtracted images in V and R bands. We assumed that the mirror image across the galactic polar axis (i.e., the flipped left-side image) as the background. We derived $V = 20.7 \pm 0.4$ and $R = 19.4 \pm 0.4$ for the SN (see §2.1), $V = 19.48 \pm 0.14$ and $R = 18.37 \pm 0.13$ for C1 and $V = 20.51 \pm 0.16$ and $R = 19.77 \pm 0.14$ for C2.
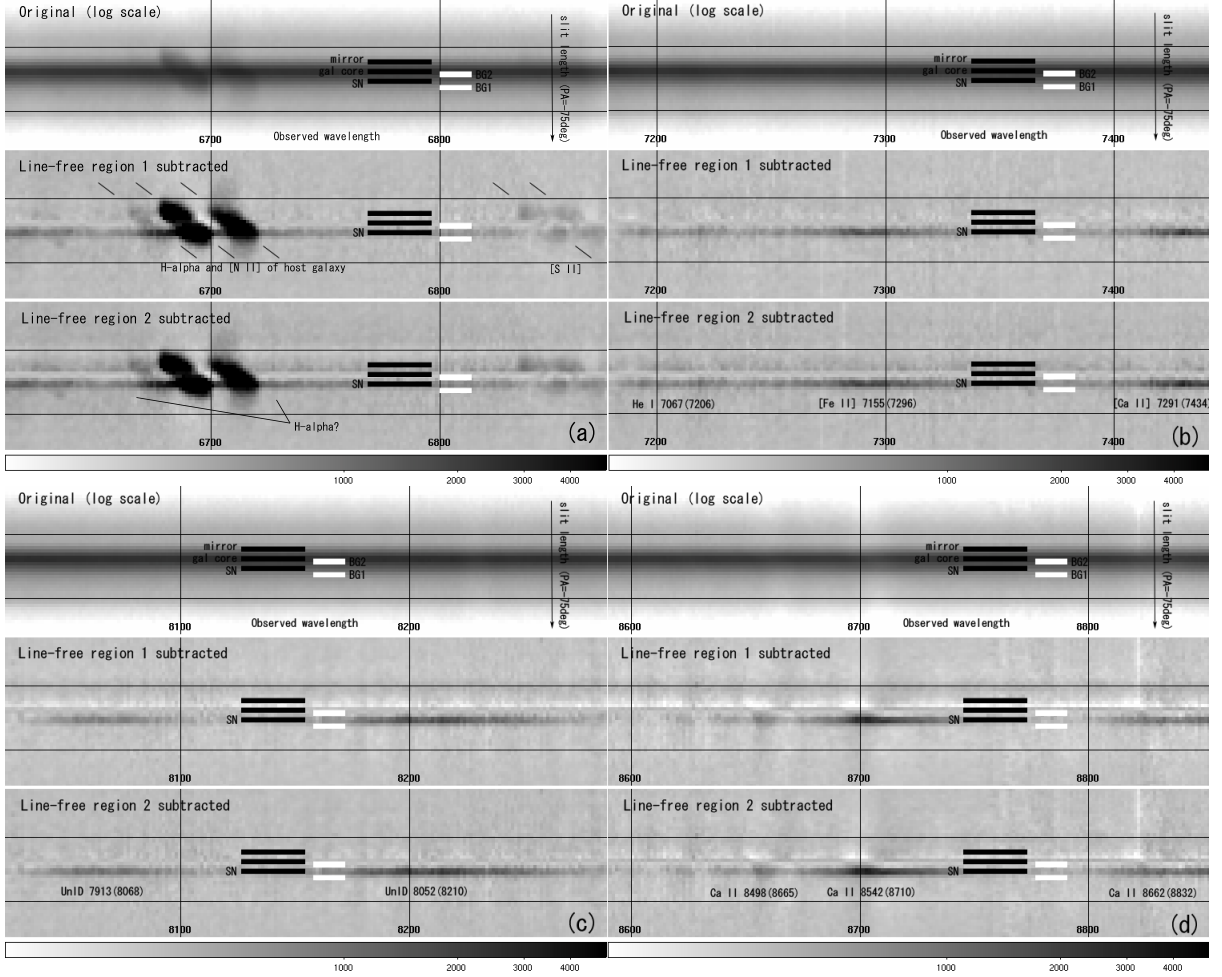
FIG. 3.— Late phase 2D spectral images around (a) 6750Å , (b) 7300Å , (c) 8150Å and 8700Å are shown (observed frame). In each wavelength region, we show (i) the original image, (ii) background (pattern 1) subtracted one and (iii) another background (pattern 2) subtracted one, from upper to lower panels. In the original image, the sky background has already been subtracted. The background pattern 1 and 2 are derived from the brightness profile along the slit (i.e., vertical axis in the panel) at apparently line-free (= pure continuum) regions for the SN, 6983–7053Å (region 1) and 7969–8011Å (region 2), respectively. Each background pattern is scaled by the galaxy core count at every wavelength bin (1 pixel) and subtracted from the original 2D spectral image. The regions used for one-dimensioning of the spectra (BG1, SN, BG2, gal core and mirror; see Fig. 4) are indicated in the panel. The width of each region is two pixels ($\simeq 0''6$). Several broad emission lines (FWHM> 50Å ~ 2000 km s^{-1}) are detected, which would be the SN origin. It should be noted that these images are shown to represent the significance of the SN spectrum even at $t = 394$ days.
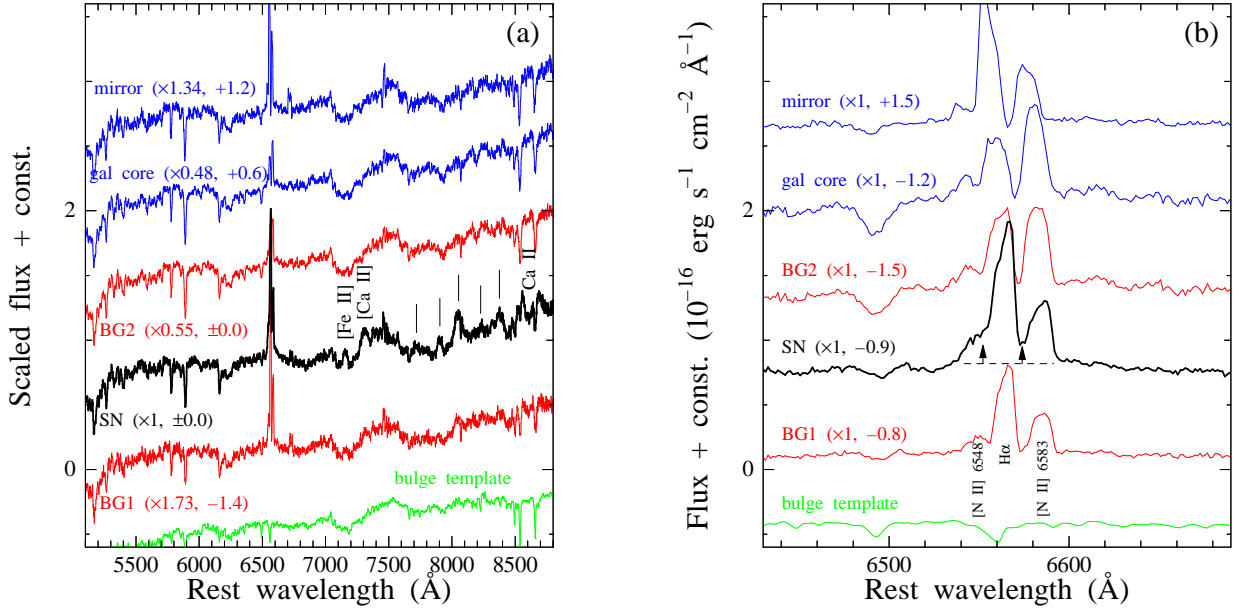
FIG. 4.— Comparison of raw spectra of the SN position and several background regions, BG1, BG2, galaxy core and mirror, at $t = 394$ days: Each spatial positions on the slit (or 2D spectrum) are shown in Fig. 1 and 3. The sky emission lines have been subtracted, but the interstellar extinction and the atmospheric absorption have not been corrected for. We also show the Bruzual & Charlot (2003) model spectrum (11 Gyr old single stellar population, solar metallicity, $A_V = 1$) as a template of slightly reddened galactic bulge for comparison. (a) Overview of the scaled spectra. All background spectra (i.e., except for the SN one) are scaled to match the SN spectrum at the line-free region, 7814–7856 Å (rest wavelength range of region 2 in Figure 3 caption). The scaling factor and the added constant for each spectrum are indicated in the panel. Some unidentified emission lines (See Table 2) are indicated by vertical lines. The weak 8050 Å emission feature seen in the scaled BG1 spectrum suggests that there is a small crosstalk of the SN component into the BG1 one. This figure shows that (i) the continuum spectra of both the SN and the background are mostly explained by the bulge component and (ii) the unidentified emission lines actually belong only to the SN position. (b) Enlarged plot of original spectra around Hα line. Most of the line fluxes are clearly from the host galaxy, which trace the galaxy rotation. However, the flux excess in the SN spectrum at the inter-line region between Hα and [N II] (indicated by arrows in the panel) imply an existence of intermediate-width Hα emission line component of $\sim 1.3 \times 10^{-17}$ erg s^{-1} cm^{-2} Å^{-1}.
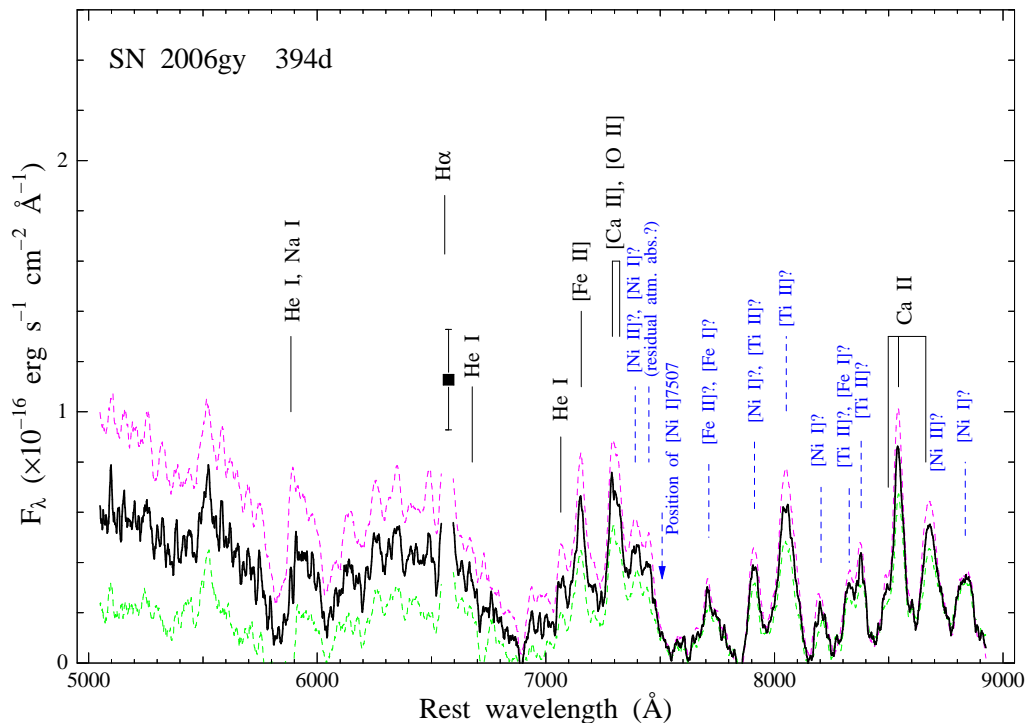
Fig. 5.— Our low resolution spectrum of SN 2006gy at $t = 394$ days, which are smoothed with neighboring eight pixels (corresponding to the width of the slit). The interstellar extinction within our galaxy and NGC 1260 have been corrected for. The atmospheric absorption bands are eliminated using the spectrum of spectrophotometric standard stars obtained on the same night. We derived this spectrum by subtraction of the average of the scaled BG1 and BG2 spectra from the SN position one (Fig. 4). The upper dashed line denotes the SN spectrum in which only the scaled BG2 is subtracted (see §2.1). On the other hand, the lower dashed line denotes that in which only the scaled BG1 is subtracted. We consider that these lines may represent the uncertainty of the derived SN spectrum. In this plot we removed the spectrum near the Hα line because its profile is distorted by the subtraction of the background H ii region component (see §2.1). Alternatively, we plotted the possible intrinsic component at Hα emission line, estimated from the residual flux at the trough between Hα and [N ii] 6584 lines (Fig. 4). There are several identified and unidentified emission lines at 7000–8800 Å, which are listed in Table 2. The position of [Ni i] 7507, which should be as strong as [Ni i] 7908, is indicated by an arrow (see §5.3).
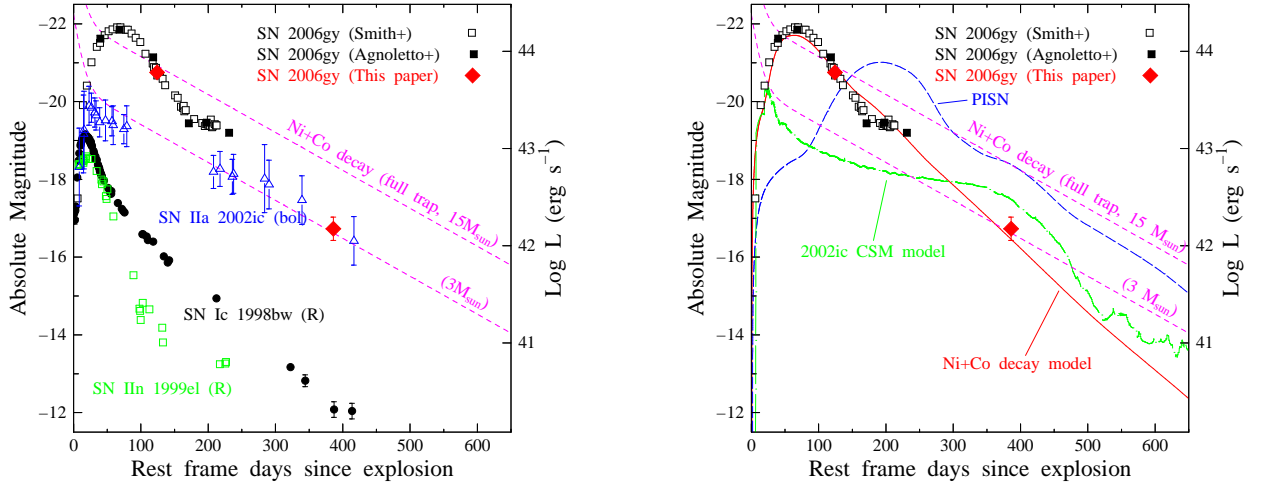
Fig. 6.— (Left) Absolute R band light curve of SN 2006gy compared with various types of SNe. For SN 2006gy, $\mu = 34.45$ and $A_R = 1.68$ are used. The right vertical axis is the luminosity assuming zero bolometric correction. Open and filled black squares are R band magnitudes of SN 2006gy by Smith et al. (2007) and Agnoletto et al. (2009), respectively. Filled red diamonds denote the R magnitude estimated from our Subaru observations. Bolometric magnitudes of SN IIa 2002ic (Deng et al. 2004), R band magnitudes of SN Ic 1998bw (Patat et al. 2001) and SN IIn 1999el (Di Carlo et al. 2002) are shown with blue open triangles, black filled circles, and green open squares, respectively. The dashed magenta lines show decay energy from $15 M_\odot$ and $3 M_\odot$ of ^{56}Ni+^{56}Co, respectively (decay data are from Nadyozhin 1994). (Right) SN 2006gy LC compared with some LC models. For LC of SN 2006gy and the dashed magenta lines are same as the left panel. Red solid line shows a synthetic LC of radioactive decay model by Nomoto et al. (2007). The parameters are $(E_K/10^{51}\text{ergs}, M_{ej}/M_\odot, M(^{56}\text{Ni})/M_\odot)$ = (64, 53, 15). This model roughly follows the overall LC from the explosion to $t = 394$ days, although the tail of the observed LC around $t = 200$ days is flatter than expected by this model. Blue dashed line denotes a model with $(E_K/10^{51}\text{ergs}, M_{ej}/M_\odot, M(^{56}\text{Ni})/M_\odot)$ = (65, 166, 15) imitating a pair-instability SN (PISN). Green dashed line is a CSM interaction model for SN 2002ic (Nomoto et al. 2005).
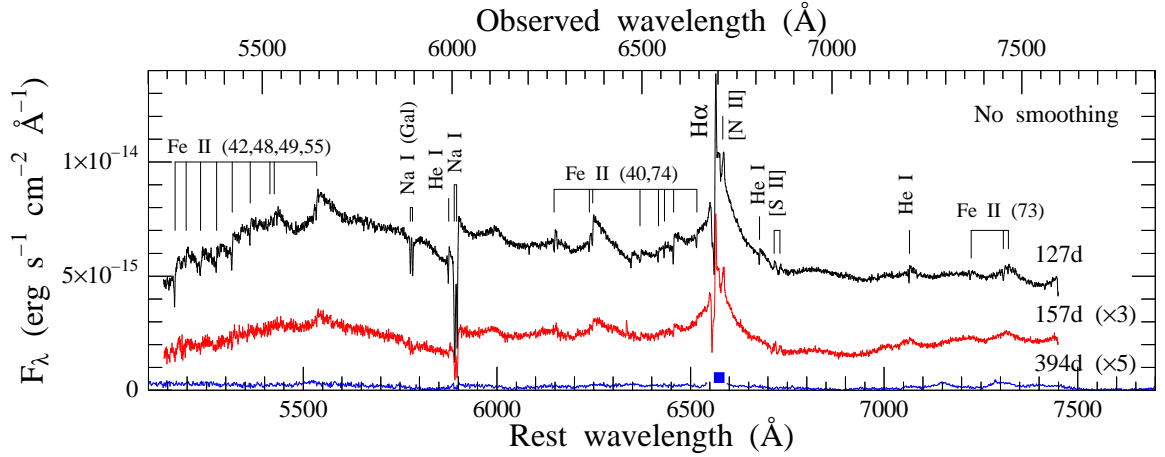

Fig. 7.— High resolution spectra of SN 2006gy at $t = 127$ and 157 days are shown together with the low resolution spectrum at 394 days. The interstellar extinction and atmospheric absorption bands have been corrected for as in Figure 5. The scaling factor of each spectrum is indicated in the panel. In the earlier spectra, Fe II, Na I, He I and Hα lines show pseudo P Cyg-like profiles with steep slope between the blue-shifted absorption and the red-shifted emission components. Most of the absorption components are much narrower than the accompanied emission lines.
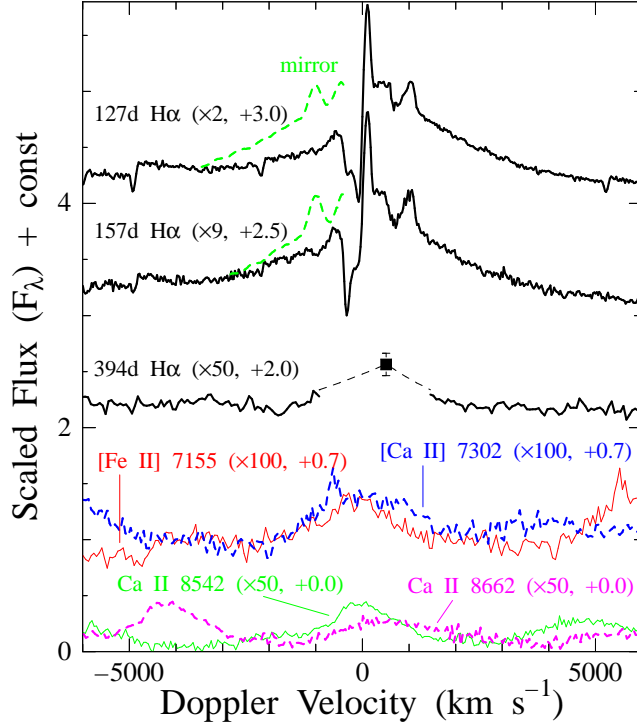
FIG. 8.— The line profiles of Hα of our three epoch spectra (black) plotted against Doppler velocity. For the spectrum at $t = 394$ days, the real profile of the Hα and [N II] lines is hardly to be known by the contamination of the background H II region components (see §2.1). Alternatively, we plot the flux at 6574 Å which is a somewhat reliable estimate from the residual flux at the trough between Hα and [N II] 6584 lines. The error bar denotes the uncertainty of its continuum level (see Fig. 5). The green dashed line labeled 'mirror' is the reflected red-side profile across $v = 0$ km s^{-1}(cf. Fig. 5 in Smith et al. 2007). The lower four lines are the Fe and Ca lines at $t = 394$ days (solid red: [Fe II] 7155, dashed blue: [Ca II] 7302 (average of 7291 and 7323), solid green: Ca II 8542, dashed magenta: Ca II 8662). The scaling factor and the added constant in each spectrum are indicated in the panel.
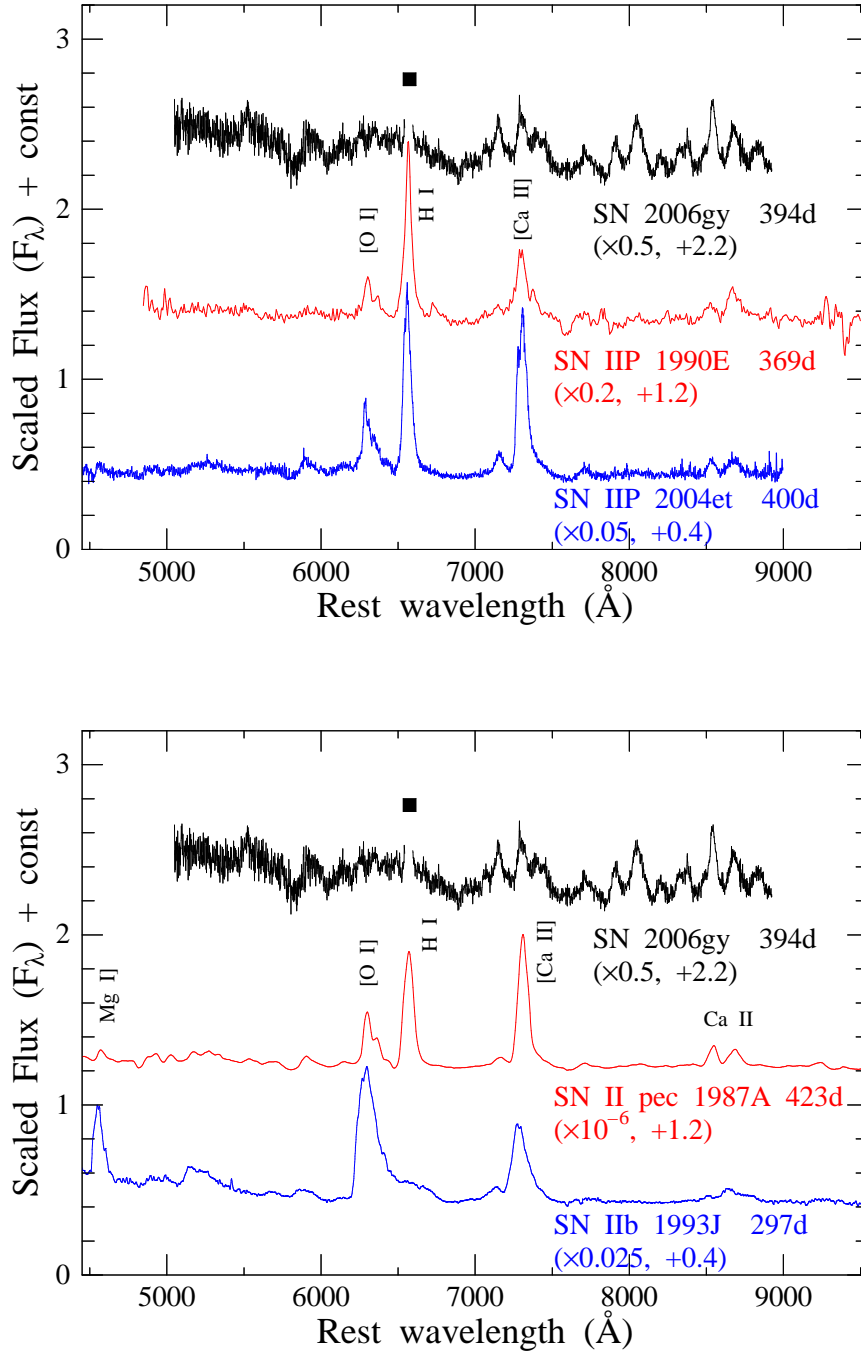
Kawabata et al.

FIG. 9.— Comparison of late time spectra with (upper panel) SNe IIP 1990E (Gómez & López 2000) and 2004et (Sahu et al. 2006) and, (lower) peculiar SN II 1987A (Pun et al. 1995) and SN IIb 1993J (Barbon et al. 1995). The unit of the vertical axis is 10^{-16} erg s^{-1} cm^{-2} Å^{-1}. Each flux is scaled and shifted for convenience of comparison and those values are indicated in the panel. The epoch is given as days from estimated explosion date (t).
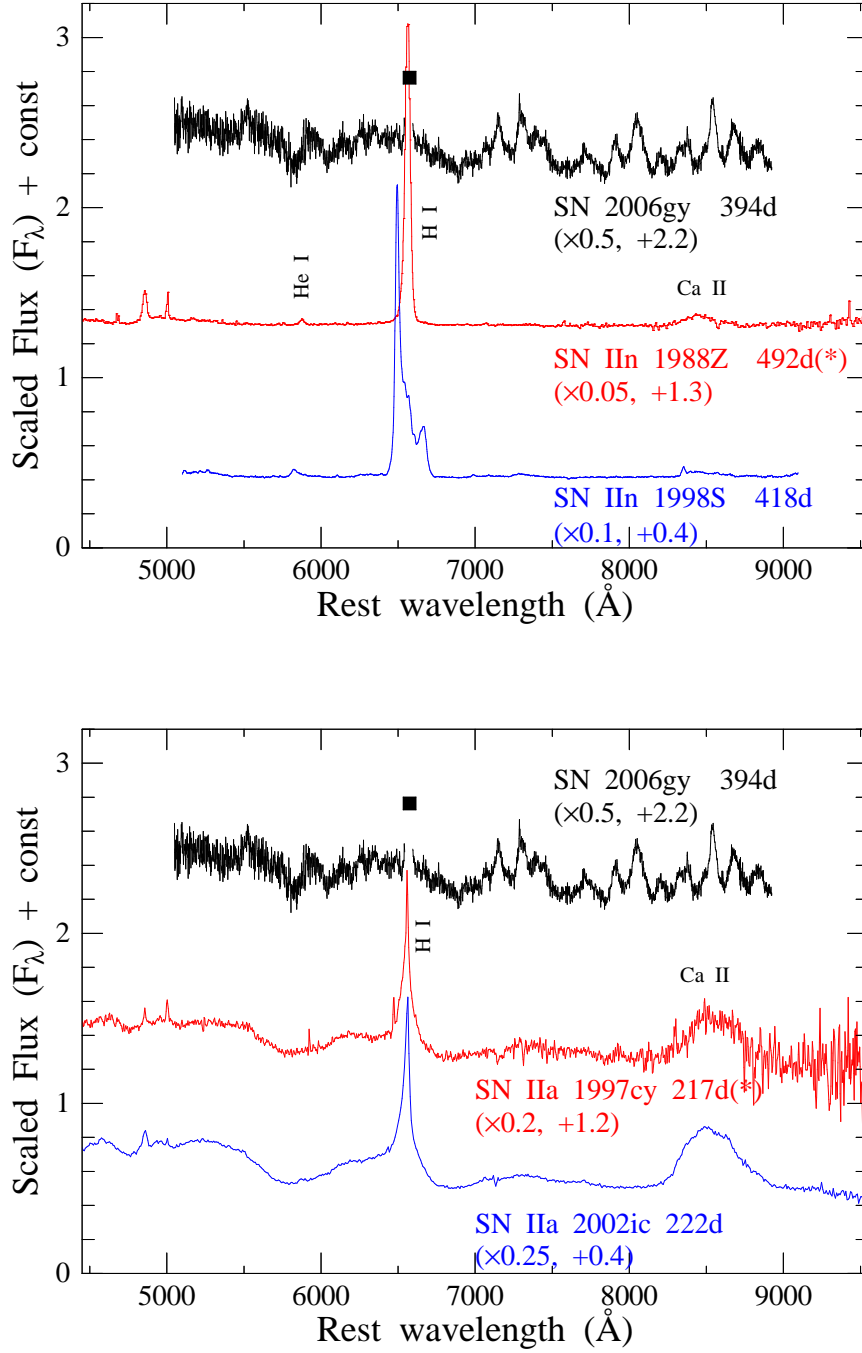
FIG. 10.— Comparison with (upper panel) SNe IIn 1988Z (Turatto et al. 1993) and 1998S (Pozzo et al. 2004), and (lower) SNe IIa 1997cy (Germany et al. 2000; Turatto et al. 2000) and 2002ic (Deng et al. 2004). The epoch is same as in Figure 9, except for SNe 1988Z and 1997cy (days since the discovery, marked with ∗). The Hα emission line of SN 1998S has a double peak profile with a wide separation.
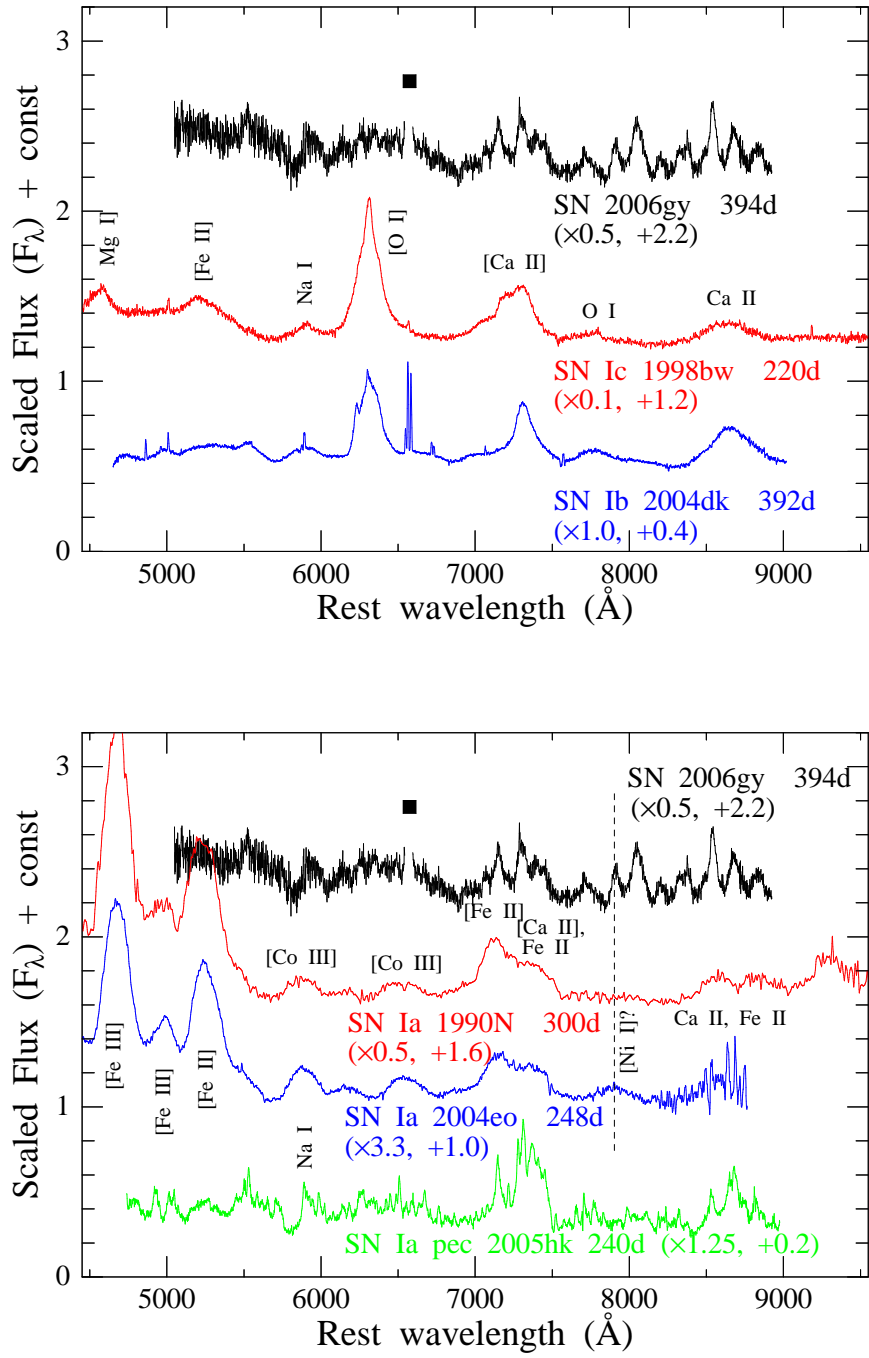
Fig. 11.— Comparison with (upper panel) SN Ic 1998bw (Patat et al. 2001) and SN Ib 2004dk (Maeda et al. 2008), and (lower) SNe Ia 1990N (Gómez & López 1998), 2004eo (Pastorello et al. 2007) and peculiar SN Ia 2005hk (Sahu et al. 2008).